Stability Analyses of Nonlinear Multivariable Feedback Control Systems

TAIN-SOU TSAY
Department of Department of Aeronautical Engineering
National Formosa University
64, Wen-Hua Road, Huwei, Yunlin
TAIWAN
tstsay@nfu.edu.tw

Abstract: - In this paper, a practical limit cycle predicting method is proposed for analyzing stability of nonlinear multivariable feedback control systems. The stable limit cycle of the considered system is found first by six criteria for unity loop gains, and then the stability is evaluated for variable loop gains. It needs only to check maximal or minimal frequency points of root-loci of equivalent gains for finding a stable limit cycle. The stability of the considered system can be classified by asymptotically stable, limit cycle and unstable regions in the parameter plane or space. The constant limit cycle loci or plane can be used as boundaries between them. Two 2x2 and two 3x3 nonlinear multivariable feedback control systems are presented to show the application of the proposed method. Calculated results are verified by digital simulations.

Key-Words: - Limit cycle predictions, Stability analysis, Nonlinear multivariable feedback control system

1 Introduction

The limit-cycle analyses play a central role for analyses and designs of nonlinear single-input single-output (SISO) or multivariable feedback control systems. In general, the stability of the considered system can be classified into asymptotically stable, limit-cycle and unstable regions in the parameter plane or space [1-4]. They can be separated by use of constant limit-cycle loci. Constant-$A_i = 0$ is the boundary between asymptotically stable and limit-cycle region. Constant-$A_i = \infty$ is the boundary between limit-cycle and unstable region. A_i are amplitudes of limit cycles.

In general, real and imaginary parts of the characteristic equation are used as two simultaneous equations to find the solution of the limit cycle for nonlinear single-input single-output (SISO) systems [5-11]. Therefore, single nonlinearity in the system can be solved easily to find two parameters; i.e., oscillation amplitude (A) and frequency (ω) of a limit cycle. The accuracy of calculation is dependent on the accuracy of equivalent gain of the nonlinearity. If two nonlinearities are dependent, then gives same conclusions.

However, nonlinearities in multivariable feedback systems are usually independent. Therefore, infinite number of solutions of limit cycles satisfies the characteristic equation for phase shifts (θ_i) between nonlinearities are not in the characteristic equation and the number of parameters to be found is always greater than two. The number of parameters to be found are $n+1$ for a $n \times n$ multivariable feedback control system with n nonlinearities in the diagonal terms; i.e., one for oscillating frequency (ω) and n for amplitudes (A_i) of inputs of n nonlinearities.

In current literature, for nonlinear multivariable systems the Nyquist, inverse Nyquist, and numerical optimization methods are usually used to predict the existence of limit cycles. These methods are based upon the graphical or numerical solutions of the linearized harmonic-balance equations [12-21]. It has been shown that, for multivariable systems, over arbitrary ranges of amplitudes (A_i), frequency (ω) and phases (θ_i), an infinite number of possible solutions may exist. Gray has proposed a sequential computational procedure to seek the solutions for only specified ranges of discrete values of A_i, ω and θ_i, these specified ranges are determined by use of Nyquist or inverse Nyquist plots [14,15]. Although the aforementioned methods are powerful, large computational efforts are usually needed. The n harmonic-balance equations include phase shifts and input amplitudes of nonlinearities will be used.

The proposed method for limit-cycle prediction is based on the parameter-plane analyses method [1-4] of the characteristic equation. Nonlinearities are replaced by sinusoidal-input describing functions (SIDFs) with fundamental components [1-4, 18-21]; i.e., quasi-linear gains. An infinite number of possible limit cycles found by real and imaginary parts of the characteristic equation and shown by root-loci in the parameter plane first. Then six criteria developed from the characteristic equation and harmonic-balance equations are used to find the unique solutions [3, 4, 15-23]. The six criteria will be deduced to check $\omega_{\max}$ or $\omega_{\min}$ points in root-loci can reduce the computation effort dramatically. Based on the found data of the stable limit-cycle for unity loop gains, the stability of the system is evaluated by use of maximal values of SIDFs of nonlinearities. The boundaries between asymptotically stable, limit-cycle and unstable regions will be found. The accuracy of calculation is dependent on the accuracy of equivalent gain of the nonlinearity [24]. Calculated results are verified by digital simulation. Runge-Kuta 4th method is used for integrations of differential equations. Possibly artificial intelligence techniques such as agent based modeling could be used to model feedback control systems and to simulate their behavior if we consider them according to the perspective of complex systems as it has been done for other complex domains such as financial markets [25].

The proposed method will be applied to one 2×2 and two 3×3 complicated nonlinear multivariable feedback control systems. It will be seen that calculated results provide accurate limit cycle predictions and stability checking of considered systems. Comparisons are made also with other methods in the current literature.

2 The Basic Approach

The limit cycle of the considered system is first found by six criteria for unity loop gains, and then the stability is evaluated for variable loop gains.

2.1 Limit cycle analyses [3, 4]

Consider the n dimensional nonlinear multivariable feedback system shown in Fig. 1. The relation between transfer function matrix $G(s)$ and nonlinearities $N(\vec{a})$ is

$$\vec{y} = G(s)N(\vec{a})K(\vec{r}-\vec{y}) \tag{1}$$

where $G(s)$ is the transfer matrix of the linear elements; $N(\vec{a})$ is the transfer matrix of equivalent gains of nonlinear elements; $K = diag([k_1\, k_2 \ldots k_n])$ is the diagonal loop gain matrix; $\vec{r}$ is the reference input vector; and $\vec{a}$ is a column vector of sinusoidal inputs to these nonlinear elements, such that

$$a_i = A_i \sin(\omega t + \theta_i),\ (i = 1,2,\ldots,n) \tag{2}$$

where A_i are amplitudes of a_i; ω is the oscillating frequency; θ_i are phase angles with respect to a reference input; and n is the dimension of the considered multivariable feedback system. The linearized harmonic-balance equations governing the existence of limit cycles can be expressed as:

$$[KG(s)N(\vec{a})+I]\vec{a}\big|_{s=j\omega} = \vec{0}, \tag{3}$$

for zero reference inputs $\vec{r}$ and $\vec{y} = -K^{-1}\vec{a}$. The determinant $\det[KG(s)N(\vec{a})+I]=0$ is the characteristic equation of the considered system. It is independent of phase angle θ_i and can be decomposed into two equations by taking real and imaginary parts for $s = j\omega$ [1-4]. The solutions need to be found for the considered nonlinear feedback control system are ($A_i,(i=1,2,..,n)$) and oscillating frequency ω of the limit cycle for a specified set of K. The number of parameters $n+1$ to be found is larger than that of two decomposed characteristic equations. It implies that there are an infinite number of solutions satisfy the characteristic equation; i.e., $\det[KG(s)N(\vec{a})+I]=0$. It needs another $n-1$ simultaneously equations. For zero inputs, Eq.(1) can be rewritten as

$$k_i \sum_{j=1}^{n}\left[\sum_{k=1}^{n} g_{ik}(s)n_{kj}(a_j)\right]a_j = -a_i \tag{4}$$

$$k_i \sum_{j=1}^{n}\left[\sum_{k=1}^{n} g_{ik}(s)n_{kj}(a_j)\right]A_j e^{j(\omega+\theta_j)} = -A_i e^{j(\omega+\theta_i)} \tag{5}$$

and

$$k_i \sum_{j=1}^{n}\left[\sum_{k=1}^{n} g_{ik}(s)n_{kj}(a_j)\right]A_j e^{j\theta_j} = -A_i e^{j\theta_i} \tag{6}$$

where $g_{ij}(s)$ is the $(i,j)^{th}$ element of $G(s)$ and $n_{kj}(a_j)$ is the $(k,j)^{th}$ element of $N(\vec{a})$. Eq.(6) represents i^{th} harmonic- balance equation. Let a_1 is the reference signal; i.e., $\theta_1 = 0$, then the another $n-1$ simultaneous equations are derived by Eq.(6) for finding solutions(i.e., $A_i,(i=1,2,..,n)$, and ω).

Note that nonlinearities in the off-diagonal and on-diagonal terms are dependent for they have same input signal. For instance, nonlinearities $(n_{i1}(a_1),(j=1,2..,n))$

are dependent for they have same input a_1 . Nonlinearities in i^{th} feedback loop, outputs of ($g_{ji}(j\omega),(j=1,2,...,n)$) and $n_{ii}(a_i)$ are dependent also. Therefore, nonlinearities in the diagonal will be discussed in this paper only.

For illustration, assume that a 2x2 nonlinear multivariable feedback system with two single-valued nonlinearities in the diagonal terms is considered. Fig.2 shows the block diagram. For $s = j\omega$, harmonic-balance equations of channel 1 and channel 2 are

$$\begin{aligned} &k_1 A_1 e^{j\theta_1} N_1(a_1) g_{11}(j\omega) \\ &\quad + k_1 A_2 e^{j\theta_2} N_2(a_2) g_{12}(j\omega) = -A_1 e^{j\theta_1} \end{aligned} \tag{7}$$

and

$$\begin{aligned} &k_2 A_1 e^{j\theta_1} N_1(a_1) g_{21}(j\omega) \\ &\quad + k_2 A_2 e^{j\theta_2} N_2(a_2) g_{22}(j\omega) = -A_2 e^{j\theta_2} \end{aligned} \tag{8}$$

respectively. Assume that the input of N_1 is the reference input (i.e., $\theta_1 = 0$), Eq.(7) gives:

$$e^{j\theta_2} = -\frac{A_1[1 + k_1 N_1(a_1) g_{11}(j\omega)]}{k_1 A_2 N_2(a_2) g_{12}(j\omega)} \tag{9}$$

and

$$\left| e^{j\theta_2} \right| \equiv M_{\theta 2} = 1 \tag{10}$$

Similarly, Eq.(8) gives

$$e^{j\theta_2} = -\frac{k_2 A_1 N_1(a_1) g_{21}(j\omega)}{A_2[1 + k_2 N_2(a_2) g_{22}(j\omega)]} \tag{11}$$

and

$$\left| e^{j\theta_2} \right| \equiv M_{\theta 2} = 1 \tag{12}$$

Equating Eqs.(9) and (11) gives

$$\begin{aligned} &1 + k_1 N_1(a_1) g_{11}(j\omega) + k_2 N_2(a_2) g_{22}(j\omega) \\ &\quad + k_1 k_2 N_1(a_1) N_2(a_2)[g_{11}(j\omega) g_{22}(j\omega) \\ &\quad - g_{12}(j\omega) g_{21}(j\omega)] = 0 \end{aligned} \tag{13}$$

Eq.(13) is the characteristic equation of the considered system in ω. It is independent on the phase angle θ_2. Eq.(13) can be expressed as

$$\begin{aligned} &1 + k_1 N_1(a_1) g_{11}(s) + k_2 N_2(a_2) g_{22}(s) \\ &\quad + k_1 k_2 N_1(a_1) N_2(a_2)[g_{11}(s) g_{22}(s) \\ &\quad - g_{12}(s) g_{21}(s)] = 0 \end{aligned} \tag{14}$$

in s-domain also. Multiplying least common multiplier (LCM) of denominators of $g_{11}(j\omega)$, $g_{22}(j\omega)$ and $\det G(j\omega)$ to Eq.(13), and taking real and imaginary parts of it, give two following equations for limit-cycle evaluation:

$$\begin{aligned} &B_1(\omega) + k_1 N_1(a_1) C_1(\omega) + k_2 N_2(a_2) D_1(\omega) \\ &\quad + k_1 k_2 N_1(a_1) N_2(a_2) E_1(\omega) = 0 \end{aligned} \tag{15}$$

and

$$\begin{aligned} &B_2(\omega) + k_1 N_1(a_1) C_2(\omega) + k_2 N_2(a_2) D_2(\omega) \\ &\quad + k_1 k_2 N_1(a_1) N_2(a_2) E_2(\omega) = 0 \end{aligned} \tag{16}$$

where $B_i(\omega), C_i(\omega), D_i(\omega), E_i(\omega)$ are polynomials of ω. They will be illustrated by a simple numerical example. Eq.(15) gives

$$N_2(a_2) = -\frac{B_1(\omega) + k_1 N_1(a_1) C_1(\omega)}{k_2[D_1(\omega) + k_1 N_1(a_1) E_1(\omega)]} \tag{17}$$

and

$$N_1(a_1) = -\frac{B_1(\omega) + k_2 N_2(a_2) D_1(\omega)}{k_1[C_1(\omega) + k_2 N_2(a_2) E_1(\omega)]} \tag{18}$$

alternatively. Eq.(16) gives

$$N_2(a_2) = -\frac{B_2(\omega) + k_1 N_1(a_1) C_2(\omega)}{k_2[D_2(\omega) + k_1 N_1(a_1) E_2(\omega)]} \tag{19}$$

and

$$N_1(a_1) = -\frac{B_2(\omega) + k_2 N_2(a_2) D_2(\omega)}{k_1[C_2(\omega) + k_2 N_2(a_2) E_2(\omega)]} \tag{20}$$

alternatively. Eqs. (17)–(20) give

$$\begin{aligned} &[C_2(\omega)E_1(\omega) - C_1(\omega)E_2(\omega)]k_1^2 N_1(a_1)^2 + [C_2(\omega)D_1(\omega) \\ &+ B_2(\omega)E_1(\omega) - C_1(\omega)D_2(\omega) - B_1(\omega)E_2(\omega)]k_1 N_1(a_1) \\ &+ [B_2(\omega)D_1(\omega) - B_1(\omega)D_2(\omega)] = 0 \end{aligned} \tag{21}$$

and

$$\begin{aligned} &[D_2(\omega)E_1(\omega) - D_1(\omega)E_2(\omega)]k_2^2 N_2(a_2)^2 + [C_1(\omega)D_2(\omega) \\ &- C_2(\omega)D_1(\omega) + B_2(\omega)E_1(\omega) - B_1(\omega)E_2(\omega)]k_2 N_2(a_2) \\ &+ [B_2(\omega)C_1(\omega) - B_1(\omega)C_2(\omega)] = 0 \end{aligned} \tag{22}$$

Note that real solutions of Eqs.(21) and (22) will be plotted in $k_1\, N_1(a_1)$ vs. $k_2\, N_2(a_2)$ plane for specified values of frequency ω. The equivalent gain of non-linearity is the sinusoidal-input describing function:

$$\begin{aligned} N_i(a_i) &= F_o + \sum_{n=1}^{\infty}(P_n + jR_n) \\ &= N_{ir}(a_i) + jN_{1i}(a_i) \end{aligned} \tag{23}$$

where

$$F_o = \frac{1}{A_i}\int_0^{2\pi} Y(t)\, d(\omega t)$$

$$P_n = \frac{1}{A_i}\int_0^{2\pi} Y(t)\cos(n\omega t)\, d(\omega t)$$

$$R_n = \frac{1}{A_i}\int_0^{2\pi} Y(t)\sin(n\omega t)\, d(\omega t)$$

and $Y(t)$ is the time function of nonlinearity with respect to input signal $A_i \sin \omega t$. Eq.(23) is a function of amplitude A_i of sinusoidal input only. Assume the nonlinearity is symmetric, then the DC component F_o is equal to zero. In general, fundamental components P_1 and R_1 are used to describe the nonlinearity [18-21]. Therefore, there is a modeling error between describing function and the real nonlinear element. It affects the accuracy of limit cycle prediction [23-24]. Consider a 2x2 plant with the transfer function matrix [3, 4, 17]:

$$G(s) = \frac{k_m}{s(s+1)^2} \begin{bmatrix} 1 & 0.3 \\ -0.2s - 0.2 & 1 \end{bmatrix} \qquad (24)$$

with $K = diag([1 \quad 1])$. Nonlinearities are two identical on-off relays with dead-zones having unity switching level (d) and unity height (M). Six criteria will be developed and illustrated by this numerical example, systematically. Describing functions with fundamental components of nonlinearities are

$$N_i(a_i) = \frac{4M}{\pi A_i}(1 - \frac{d^2}{A_i^2})^{1/2}, \quad A_i \ge d, i = 1,2 \qquad (25)$$

where $M = 1$ and $d = 1$. It is a single-value nonlinearities. The characteristic equation of the closed-loop system in s-domain is

$$\begin{aligned} &s^6 + 4s^5 + 6s^4 + 4s^3 + s^2 + k_m N_1(a_1)(s^3 + 2s^2 + s) \\ &+ k_m N_2(a_2)(s^3 + 2s^2 + s) \\ &+ k_m^2 N_1(a_1) N_2(a_2)(0.006s + 1.06) = 0 \end{aligned} \qquad (26)$$

Real and imaginary parts of Eq.(26) for $s = j\omega$ are

$$\begin{aligned} &-\omega^6 + 6\omega^4 - \omega^2 + k_m N_1(a_1)(-2\omega^2) \\ &\quad + k_m N_2(a_2)(-2\omega^2) + k_m^2 N_1(a_1) N_2(a_2)(1.06) = 0 \end{aligned} \qquad (27)$$

and

$$\begin{aligned} &4\omega^5 - 4\omega^3 + k_m N_1(a_1)(-\omega^3 + \omega) \\ &+ k_m N_2(a_2)(-\omega^3 + \omega) + k_m^2 N_1(a_1) N_2(a_2)(0.06\omega) = 0 \end{aligned} \qquad (28)$$

For $k_m = 3$, the root-loci (in Fig.3) show there are an infinite sets of possible solutions ($N_1(a_1), N_2(a_2), \omega$) satisfy Eqs.(27) and (28). However, only one set of solution ($N_1(a_1), N_2(a_2), \omega$) satisfies for the considered system; i.e., stable limit-cycle. Other solutions are called as “unstable limit-cycle”. Therefore, criteria for checking the existence of a stable limit-cycle must be developed.

By use of Fig.3, six criteria of the system having a stable limit cycle are developed and explained as follows:

Criterion 1: Every point on the root-loci evaluated by Eqs. (27) and (28), as shown in Fig.3, represents a set of $N_1(a_1)$, $N_2(a_2)$ and ω, which can satisfy the condition of having a limit cycle. Note that infinite possible solutions are found.

Criterion 2: A limit cycle may exist only if the values of $N_i(a_i)$ are less than the maximal gain $N_i(a_i)_{\max}$ of nonlinearities N_i. Now, possible solutions of limit-cycle are reduced on the segment of the root-loci between points Q_2 and Q_3 only.

Criterion 3: If the root-loci separate the stable and unstable regions, then a stable limit cycle may exist at the root-loci. The reason is that the system will become stable (unstable) when amplitude A_i increase (decrease). In other words, the system becomes stable (unstable) when the amplitude A_i increase (decrease), a stable limit cycle may exist on the stability boundary; i.e., on the root-loci. The descriptions of a stable limit cycle can be expressed mathematically by the following equation [4]:

$$\frac{\partial \sigma}{\partial A_i} = \left(\frac{\partial \sigma}{\partial N_i(a_i)} \right) \left(\frac{\partial N_i(a_i)}{\partial A_i} \right) < 0, \ i = 1,2 \qquad (29)$$

Note that $\partial N_i(a_i) / \partial A_i$ of Eq.(19) can be evaluated as

$$\frac{\partial N_i(a_i)}{\partial A_i} = \frac{4M}{\pi A_i^2} \left[-(1 - \frac{d^2}{A_i^2})^{1/2} + \frac{d^2}{A_i^2}(1 - \frac{d^2}{A_i^2})^{-1/2} \right] \qquad (30)$$

Criteria 1 to 3 give possible solutions of a stable limit cycle are at segment of the locus between Q_2 and Q_3; i.e., give ranges of frequency ω and $N_i(a_i)$. But it still has an infinite number of solutions.

Criterion 4: A stable limit-cycle exists only for phase angles found by Eqs.(9) and (11) are equal to each other; i.e.,

$$\theta_2^{\{9\}} - \theta_2^{\{11\}} = 0 \qquad (31)$$

where $\theta_2^{\{9\}}$ and $\theta_2^{\{11\}}$ represent phase angles found by Eqs.(9) and (11), respectively. This criterion will reduce the number of possible solutions of limit cycles.

Criterion 5: A stable limit-cycle exists only for magnitudes found by Eqs.(10) and (12) are equal; i.e.,

$$M_{\theta 2}^{\{10\}} - M_{\theta 2}^{\{12\}} = 0 \qquad (32)$$

Note that Eqs.(9) and (11) give magnitudes of them are equal to unities; i.e., represented by Eqs.(10) and

(12). Note that a rule of thumb for expects value of $M_{\theta 2}$ greater than 0.80 is used in this paper. Two correction equations will be developed to correct the mathematical errors of describing functions with fundamental components. Criteria 4 and 5 reduced the number of possible solutions. Next criterion will be developed for finding unique solution.

Criterion 6: The unique solution of a stable limit cycle is at the unique frequency point of the root-locus; i.e., the solutions of Eq.(21) for $N_1(a_1)$ are real and equal to each other. This condition gives

$$\begin{aligned}&[C_2(\omega)D_1(\omega)+B_2(\omega)E_1(\omega)-C_1(\omega)D_2(\omega)-B_1(\omega)E_2(\omega)]^2\\&-4[C_2(\omega)E_1(\omega)-C_1(\omega)E_2(\omega)][B_2(\omega)D_1(\omega)\\&-B_1(\omega)D_2(\omega)]=0\end{aligned} \tag{33}$$

Similar equation can be derived for $N_2(a_2)$ with Eq.(22). Fig.3 shows the maximal frequency $\omega_{\max}$ of the found upper root-locus is 1.38823 rad/s at point $Q_0(1.5041,1.5041)$; and the minimal frequency $\omega_{\min}$ of the lower root-locus is 0.7888017 rad/s at Point $Q_1(0.3803,0.3803)$. Q_0 is a impossible solution for it violates ***Criteria*** 2 and 3. Q_1 is the unique solution satisfies criteria 2~5 and Eq.(33). Therefore, the unique solution is found.

From the root-loci shown in Fig.3, Eq.(33) can be described by a graphical rule also. it is

$$\frac{\partial N_i(a_i)}{\partial \omega}=0 \tag{34}$$

Eq.(34) represents the departure point $\omega_{\min}$ (point Q_1 in Fig.3) of the root-locus with respect to the frequency ω, or the approaching point $\omega_{\max}$ (Point Q_0 in Fig.3) of root-locus.

If the solution satisfies all six criteria for a stable limit cycle, then a stable limit cycle will exist. Table 1 gives calculated results of Point Q_1. Two sets of (A_1, A_2) satisfy found $N_1(a_1)$ and $N_2(a_2)$. First set of $(A_1, A_2)=(3.178,3.178)$ is the desired solutions. Second set of $(A_1, A_2)=(1.054,1.054)$ is impossible for its $\partial N_1(a_1)/\partial A_1$ and $\partial N_2(a_2)/\partial A_2$ violate ***Criterion*** 3. Calculated results for Q_3 are given in Table 1 also for illustrating it is an unstable limit cycle.

Note that (A_i) are found from Eq.(25); i.e., describing function of the relay with dead band, therefore $M_{\theta 2}$ found by Eq.(10) or Eq.(12) are usually not equal to unities for mathematical errors of the nonlinearities. By multiplying a scaling factor S_k to left and right side of Eq.(10) for $|e^{-j\theta 2}|=1$, then Eq.(10) becomes

$$S_k\left(\frac{A_1}{A_2}\right)\left|\frac{1+N_1(a_1)g_{11}(j\omega)}{k_1N_2(a_2)g_{12}(j\omega)}\right|\equiv S_kM_{\theta 2}=1 \tag{35}$$

An approximate formulation for S_k is

$$S_k\approx\frac{1+(1-M_{\theta 2})/2}{1-(1-M_{\theta 2})/2}=\frac{1.5-0.5M_{\theta 2}}{0.5+0.5M_{\theta 2}} \tag{36}$$

The error of $S_kM_{\theta 2}-1$ is less than 0.5% for 0.9< $M_{\theta 2}$ <1.1(1.2% for 0.85 < $M_{\theta 2}$ <1.15). Eqs.(35) and (36) give the modified values (A_{im}) of (A_i) are

$$A_{1m}=A_1[1+(1-M_{\theta 2})/2]=A_1(1.5-0.5M_{\theta 2}) \tag{37}$$

and

$$A_{2m}=A_2[1-(1-M_{\theta 2})/2]=A_2(0.5+0.5M_{\theta 2}) \tag{38}$$

Using Eqs.(37) and (38), the modified values are $A_{1m}=3.3023$ and $A_{2m}=3.0527$. Fig.4 shows simulation verification result of the considered system in which gives $A_1=3{,}309$, $A_2=3.032$, $\omega=0.790 rad/s$, and $\theta_2=-70.56°$. They give that calculated results corrected by Eqs.(37) and (38) give accurate prediction of the stable limit cycle.

If k_m is an adjustable parameter, then the minimal value of k_m just having a stable limit cycle can be found by the same evaluating procedures and criteria. The found value is 1.7915. The root-locus for k_m =1.7915 is shown in Fig.5. It implies that there will have no intersection between root-locus and constant $N_1(a_1)_{\max}$, and $N_2(a_2)_{\max}$ lines. The system is asymptotically stable for k_m is less than 1.7915. Therefore, the proposed method can be used for designing nonlinear multivariable feedback control systems also; i.e., not only for analyses. The comparisons with other methods [17] for minimal k_m are given in Table 2.

Six criteria for finding a stable-limit cycle have been developed for nonlinear multivariable feedback control system. Note that six criteria are deduced to check the $\omega_{\max}$ or $\omega_{\min}$ point of root-loci which satisfies criteria 2 to 5. This reduces the computing effort dramatically.

2.2 Stability Analyses method

In this subsection, method for finding boundaries between asymptotically stable and limit-cycle is developed. The boundaries between asymptotically stable and unstable region are classified by constant limit-cycle locus $A_i = 0$. The boundaries will be illustrated in k_1 vs. k_2 planes for 2x2 systems. Consider the illustrating plant described by Eq.(18) with $k_m = 3$ and $K = [k_1 \quad k_2]$; and nonlinearities described by Eq.(25); Eq.(26) can be rewritten as

$$\begin{aligned} &s^6 + 4s^5 + 6s^4 + 4s^3 + s^2 + k_1 N_1(a_1)(s^3 + 2s^2 + s) \\ &+ k_2 N_2(a_2)(s^3 + 2s^2 + s) \\ &+ k_1 k_2 N_1(a_1) N_2(a_2)(0.006s + 1.06) = 0 \end{aligned} ; \quad (42)$$

Let $k_1 N_1(a_1)$ and $k_2 N_2(a_2)$ are two parameters to be analyses, then root-loci for possible solutions are shown in Fig.6. Similar to the last conclusion for existence of a stable limit cycle, $Q_4(0.3803, 0.3803)$ represents the only solution for stable limit cycle. The maximal frequency (ω_{max}) is 0.7888rad/s. The Criterion 2 gives

$$k_1 N_1(a_1)_{max} \geq 0.3803; \quad (43)$$

and

$$k_2 N_2(a_2)_{max} \geq 0.3803; \quad (44)$$

Eqs.(43) and (44) give $k_1 \geq 0.5974 \; and \; k_2 \geq 0.5974$ for $N_1(a_1)_{max} = 0.6366$ and $N_2(a_2)_{max} = 0.6366$. The value 0.5974 represents the boundary between limit-cycle and asymptotically stable regions. The simulation verification gives 0.597. Table 3 gives calculated and simulated results for variable set of (k_1, k_2). Amplitudes (A_1, A_2) are found by $N_1(a_1) = 0.3803/k_1$, $N_2(a_2) = 0.3803/k_2$ and Eq.(25). It can be seen that calculated results are quite close to simulated results.

Note that one can choose parameters in the asymptotically region to get wanted system performance, or choose parameters in the limit-cycle region to get wanted oscillation condition[2]. The proposed method is ready to be applied to real systems. The proposed method will be applied to one 2x2 and two 3x3 nonlinear multivariable feedback control systems in the next section. Nonlinearities considered are saturation, saturation with dead-zone, Bang-Bang, and Bang-Bang with dead-zone. They are general characteristics of controllers realized by power limited electrical RLC, BJT, and MOS network[1-4, 26-27].

3. Numerical Examples

Example 1. Consider a nonlinear multivariable system with transfer function matrix [28]

$$G(s) = \begin{bmatrix} \dfrac{12.8e^{-s}}{16.7s+1} & \dfrac{18.9e^{-3s}}{21s+1} \\ \dfrac{6.6e^{-7s}}{10.9s+1} & \dfrac{19.4e^{-3s}}{14.4s+1} \end{bmatrix} \quad (45)$$

Two nonlinearities are shown in Fig.7. Similar to the procedure stated in Section 2.1, the found root-loci are shown in Fig.8. There are two ω_{max} (Q_6, Q_8) and two ω_{min} (Q_5, Q_7) points of root-loci. They represent possible solutions of the stable limit cycle. But only the $Q_5(0.4541, 0.2929)$ is the solution for it satisfies criterion 2 to 5. The ω_{min} is equal to 0.4875 rad/s. The simulation verification is shown in Fig.9. Comparison of the calculated and simulated results is given in Table 4. It can be seen that calculated results give accurate prediction of the considered system. Note that the transportation lag is a periodic function of frequency ω. Therefore, Fig.8 gives four maximal and minimal frequency points of root-loci. Example 1 gives the proposed method give an effect way to find the exact solution.

Now considers the stability of the considered system for $K = diag[k_1, k_2]$. The Criterion 2 gives

$$k_1 N_1(a_1)_{max} \geq 0.4541; \quad (46)$$

and

$$k_2 N_2(a_2)_{max} \geq 0.2929; \quad (47)$$

Eqs.(46) and (47) give $k_1 \geq 0.4541 \; and \; k_2 \geq 0.3709$ for $N_1(a_1)_{max} = 1$ and $N_2(a_2)_{max} = 0.7897$. $k_1 = 0.4541$ and $k_2 = 0.3709$ are boundaries between asymptotically stable and limit-cycle regions. Note that there is no unstable region. The calculated and simulated results for other sets of (k_1, k_2) are given in Table 5. It can be seen that calculated results are quite close to simulated results.

Example 2. Consider a 3x3 multivariable process [29] given by

$$G(s) = \frac{2e^{-s}}{s^2 + 1.1s + 0.1} \begin{bmatrix} -0.4s - 0.4 & 3s + 0.3 & 2s + 0.2 \\ 3s + 0.3 & 2s + 0.2 & -0.4s - 0.4 \\ 2s + 0.2 & -0.4s - 0.4 & 3s + 0.3 \end{bmatrix} \quad (48)$$

There are three relay nonlinearities in the diagonal terms. The magnitude (M) of each nonlinearity is 1.0. Describing functions of them are

$$N_i(a_i) = \frac{4M}{\pi A_i}, i = 1,2,3 \quad (49)$$

Harmonic-balance equations of the system are given by

$$\begin{bmatrix} 1+k_1N_1(a_1)g_{11}(s) & k_1N_2(a_2)g_{12}(s) & k_1N_3(a_3)g_{13}(s) \\ k_2N_1(a_1)g_{21}(s) & 1+k_2N_2(a_2)g_{22}(s) & k_2N_3(a_3)g_{23}(s) \\ k_3N_1(a_1)g_{31}(s) & k_3N_2(a_2)g_{32}(s) & 1+k_3N_3(a_3)g_{33}(s) \end{bmatrix} \begin{bmatrix} A_1e^{j\theta_1} \\ A_2e^{j\theta_2} \\ A_3e^{j\theta_3} \end{bmatrix} = \vec{0} \tag{50}$$

where $g_{ij}(s)$ is the $(i,j)^{th}$ element of G(s). For given A_1 and $\theta_1=0$ as a reference phase, $e^{j\theta_2}$ and $e^{j\theta_3}$ can be found by following equations:

$$\begin{bmatrix} e^{j\theta_2} \\ e^{j\theta_3} \end{bmatrix} = \begin{bmatrix} A_2k_1N_2(a_2)g_{12}(s) & A_3k_1N_3(a_3)g_{13}(s) \\ A_2[1+k_2N_2(a_2)g_{22}(s)] & A_3k_2N_3(a_3)g_{23}(s) \end{bmatrix}^{-1} \times \begin{bmatrix} -A_1[1+k_1N_1(a_1)g_{11}(s)] \\ -A_1k_2N_1(a_1)g_{21}(s) \end{bmatrix} \tag{51}$$

$$\begin{bmatrix} e^{j\theta_2} \\ e^{j\theta_3} \end{bmatrix} = \begin{bmatrix} A_2k_1N_2(a_2)g_{12}(s) & A_3k_1N_3(a_3)g_{13}(s) \\ A_2k_3N_2(a_2)g_{32}(s)] & A_3[1+k_3N_3(a_3)g_{33}(s)] \end{bmatrix}^{-1} \times \begin{bmatrix} -A_1[1+k_1N_1(a_1)g_{11}(s)] \\ -A_1k_3N_1(a_1)g_{31}(s) \end{bmatrix} \tag{52}$$

and

$$\begin{bmatrix} e^{j\theta_2} \\ e^{j\theta_3} \end{bmatrix} = \begin{bmatrix} A_2[1+k_2N_2(a_2)g_{22}(s)] & A_3k_2N_3(a_3)g_{23}(s) \\ A_2k_2N_2(a_2)g_{32}(s) & A_3[1+k_3N_3(a_3)g_{33}(s)] \end{bmatrix}^{-1} \times \begin{bmatrix} -A_1k_2N_1(a_1)g_{21}(s) \\ -A_1k_3N_1(a_1)g_{31}(s) \end{bmatrix} \tag{53}$$

alternatively.

$$e^{j\theta_2(51)} = e^{j\theta_2(52)} = e^{j\theta_2(53)} \tag{54}$$

$$e^{j\theta_3(51)} = e^{j\theta_3(52)} = e^{j\theta_3(53)} \tag{55}$$

For $k_1=k_2=k_3=1$, Eq.(50) gives the characteristic equation of the system:

$$\begin{aligned} &1+k_1N_1(a_1)g_{11}(s)+k_2N_2(a_2)g_{22}(s)+k_3N_3(a_3)g_{33}(s) \\ &+k_1k_2N_1(a_1)N_2(a_2)[g_{11}(s)g_{22}(s)-g_{12}(s)g_{21}(s)] \\ &+k_1k_3N_1(a_1)N_3(a_3)[g_{11}(s)g_{33}(s)-g_{13}(s)g_{31}(s)] \\ &+k_2k_3N_2(a_2)N_3(a_3)[g_{22}(s)g_{33}(s)-g_{23}(s)g_{32}(s)] \\ &+k_1k_2k_3N_1(a_1)N_2(a_2)N_3(a_3)D_{g(}s)=0; \end{aligned} \tag{56}$$

where $D_g(s)$ represents the determinant of the transfer function matrix G(s).

For $k_1=k_2=k_3=1$ and a specified value of $N_3(a_3)$, the characteristic equation is function of $N_1(a_1)$, $N_2(a_2)$ and ω only. Eq.(56) can be written as in the form of

$$\begin{aligned} &1+N_3(a_3)g_{33}(s)+\{g_{11}(s)+N_3(a_3)[g_{11}(s)g_{33}(s) \\ &-g_{13}(s)g_{31}(s)]\}N_1(a_1)+\{g_{22}(s)+N_3(a_3)[g_{22}(s)g_{33}(s) \\ &-g_{32}(s)g_{23}(s)]\}N_2(a_2)+\{g_{11}(s)g_{22}(s)-g_{12}(s)g_{21}(s) \\ &+N_3(a_3)D_g(s)\}N_1(a_1)N_2(a_2)=0 \end{aligned} \tag{57}$$

Therefore, same analyzing procedures for 2x2 non-linear multivariable systems described by Eqs.(13)-(22) and six criteria can be applied. Fig.10 shows parameter analyses of several constant-$N_3(a_3)$ loci. Each constant-$N_3(a_3)$ locus shows the maximal frequency $\omega_{\max}$. Intersecting points between the dot line and constant-$N_3(a_3)$ loci give $\omega_{\max}$ of constant-$N_3(a_3)$ loci. It gives the maximal frequency with respect to $N_3(a_3)$ is $\omega_{\max}=2.061 rad/s$ at $N_3(a_3)=0.499$. Corresponding values of $N_i(a_i)$ are the point $Q_9(0.498,0.499)$. It is the unique solution of the stable limit cycle. The found A_i are $(A_1,A_2,A_3)=(2.559, 2.552,2.552)$. They are found by inverting the describing functions. Fig.11 shows simulation results in which gives $(A_1,A_2,A_3)=$ $(2.836,2.836,2.836)$ and $\omega=2.145 rad/s$. Since $N_i(a_i)_{\max}=\infty$, therefore limit cycle is always exist for $k_i>\mathbf{0}$. Calculated and simulated results for other set (k_1,k_2,k_3) are given in Table 6. It can be seen that calculated results are quite closed to simulated results for this nonlinear 3x3 multi-variable feedback control system.

Example 3. Consider a 3x3 multivariable feedback control system with the transfer function matrix [30]

$$G(s)=\begin{bmatrix} \dfrac{11.9e^{-5s}}{21.7s+1} & \dfrac{4e^{-5s}}{337s+1} & \dfrac{0.21e^{-5s}}{10s+1} \\ \dfrac{7.7e^{-5s}}{50s+1} & \dfrac{7.67e^{-3s}}{28s+1} & \dfrac{0.5e^{-5s}}{10s+1} \\ \dfrac{9.3e^{-5s}}{50s+1} & \dfrac{-3.67e^{-5s}}{166s+1} & \dfrac{10.33e^{-4s}}{25s+1} \end{bmatrix} \tag{58}$$

There are three nonlinearities on the diagonal. Fig.12 shows the nonlinearities. Fig.13(a) shows root-loci of possible solutions of limit cycles in the $N_1(a_1)$ vs. $N_2(a_2)$ plane for specified values of $N_3(a_3)$. The $\omega_{\max}$-locus shows connections of each $\omega_{\max}$ point of constant-$N_3(a_3)$ locus. The maximal value of the $\omega_{\max}$- locus shown in Fig.13(b) gives $\omega_{\max}=0.3593 rad/s$; i.e., point Q_{11}. The point Q_{11} represents existence of a stable limit cycle; i.e., $\omega=0.3593 rad/s$, $N_1(a_1)=0.6578$, $N_2(a_2)=1.6919$ and $N_3(a_3)=0.91$. Corresponding amplitudes are $A_{1c}=1.835$, $A_{2c}=0.8684$ and $A_{3c}=1.2215$. They are found by inverting the describing functions. Fig.14 shows digital simulations in which gives $A_{1s}=1.976$, $A_{2s}=0.8769$, $A_{3s}=1.292$ and $\omega=0.361 rad/s$. It shows calculated results are closed to simulated results.

Now considers the stability of the considered system for $K = diag[k_1, k_2, k_3]$.The Criterion 2 gives

$$k_1 N_1(a_1)_{\max} \geq 0.6578; \quad (59)$$

$$k_2 N_2(a_2)_{\max} \geq 1.6919; \quad (60)$$

and

$$k_3 N_3(a_3)_{\max} \geq 0.910; \quad (61)$$

Eqs.(59)-(61) give $k_1 \geq 0.6578, k_2 \geq 0.8177$ and $k_3 \geq 0.91$ for $N_1(a_1)_{\max} = 1$, $N_2(a_2)_{\max} = 2.069$ and $N_3(a_3)_{\max} = 1$. $k_1 = 0.6578, k_2 = 0.8177$ and $k_3 = 0.91$ are boundaries between asymptotically stable and limit-cycle regions. The digital simulation gives $k_1 = 0.6285$, $k_2 = 0.783$ and $k_3 = 0.856$

4. Conclusions

The limit-cycle prediction method has been proposed to find the stability of nonlinear multivariable feedback control systems. It needs only to check maximal or minimal frequency points of root-loci of equivalent gains for finding a stable limit cycle. Based on the found stable limit cycle, the stability of the system can be found easily. Two 2x2 and two 3x3 complicated nonlinear multivariable feedback control examples give the proposed method provides an effect way to find limit cycles and stability boundaries.

References:

[1] T. S. Tsay, Load frequency control of interconnected power system with governor backlash nonlinearities, International Journal of Electrical Power and Energy System, Vol.33, 2011**,** pp.1542-1549.

[2] T. S. Tsay, Analyses and designs of a nonlinear mechanical scanning control system, Journal of the Franklin Institute, Vol. 343, no.1, 2006, pp. 83-93.

[3] T. S. Tsay and K. W. Han, Limit cycle analysis of nonlinear multivariable feedback control systems, Journal of the Franklin Institute, Vol.325, no.6, 1988, pp.721-730.

[4] T. S. Tsay, Limit Cycle Predictions for nonlinear multivariable feedback control systems with large transportation lags, Journal of Control Science and Engineering, Vol.2011, Article ID169848, 2011, p.11.

[5] M. Basso, R. Genesio and A. Tesi, A frequency method for predicting limit cycle bifurcations, Nonlinear Dynamics, Vol.13, no.4, 1997, pp.339-360.

[6] B. F. Wu and S.M. Chang, A stabilized analysis of a front-wheel-steered vehicle with simulated trajectories, WSEAS Transactions on SYSTEMS, Vol.6, no.6, 2007, pp.1138-1146.

[7] P. S. V. Nataraj and J. J. Brav, Reliable and accurate algorithm to computer the limit cycle locus for uncertain nonlinear system, IEE Proceedings on Control Theory and Applications, Vol.150, no.5, 2003, pp.457-466.

[8] B. F. Wu, J. W. Perng, H. I. Chin, Existence and uniqueness of limit cycle for a class of nonlinear discrete-time systems, Chaos, Solitons & Fractals, Vol.38, no.1, 2008, pp.89-96.

[9] V. K. Pillai and H. D. Nelson, A new algorithm for limit cycle analysis of nonlinear control systems, J. Dynamic Systems, Measurement, and Control, Vol.110, no.3, 1988, pp.272–277.

[10]B. F. Wu, H. I. Chin and J.W. Perng, Gain-phase margin analysis of nonlinear perturbed vehicle control systems for limit cycle prediction, WSEAS Transaction on System, Vol.3,no.5, 2004, pp.1881-1886.

[11]Y. J. Wang, Robust prevention of limit cycle for nonlinear control systems with parametric uncertainties both in the linear plant and nonlinearity, ISA Transactions, Vol.46, no.4, 2007, pp.479-491.

[12]K. C. Patra and Y. P. Singh, Graphical method of prediction of limit cycle for multivariable nonlinear systems, IEE Proceedings on Control Theory and Applications, Vol.143, no.5, 1996, pp. 423-428.

[13]J. O. Gray and P. M. Taylor, Computer aided design of multivariable nonlinear control systems using frequency domain techniques, Automatica, Vol.15, no.3, 1979, pp. 281-297.

[14]J. O. Gray and N. B. Nakhla, Prediction of limit cycles in multivariable nonlinear systems, IEE Proceedings on Control Theory and Applications, Vol.128, no.5, 1981, pp.233-241.

[15]H. Chang, C. Pan, C. Huang, C. Wei, A general approach for constructing the limit cycle loci of multiple-nonlinearity systems, IEEE Transaction on Automatic Control, Vol.32, no.8, 1987, pp.845-848 .

[16]F. Paoletti, A. Landi and M. A. Innocentti, A CAD tool for limit cycle prediction in nonlinear systems, IEEE Transactions on Education, Vol.39, no.4, 1996, pp.505–511.

[17]S. D. Katebi and M. R. Katebi, Control design for multivariable multivalued nonlinear systems, Systems Analysis Modelling Simulation, Vol.15, no.1, 1994, pp.13–37.

[18]D. P. Atherton, Nonlinear control engineering, Van Nostrand Reihold Co., London & New York, 1982.

[19]J. H. Taylor, Describing functions, in Electrical Engineering Encyclopaedia, John Wiley & Sons, New York, USA, 1999.

[20]D. P. Atherton and S. Spurgeon, Nonlinear control systems,analytical methods, Electrical Engineering Encyclopaedia, John Wiley & Sons, Inc. New York, 1999.
[21]H. Khalil, Nonlinear systems, Prentice-Hall, Upper Saddle River, NJ, 3rd edition, 2002.
[22]Y. J. Sun, Existence and uniqueness of limit cycle for a class of nonlinear discrete-time systems, Chaos, Solitons & Fractals, Vol.38, no.1, 2008, pp.89-96.
[23]C. Lin and Q. G. Wang, On uniqueness of solutions to relay feedback systems, Automatica, Vol.38, no.1, 2002, pp.177-180.
[24]S. Engelberg, Limitation of the describing function for limit cycle prediction, IEEE Transaction on Automatic Control, Vol.47, no.11, 2002, pp.1887-1890.
[25]F. Neri , A comparative study of a financial agent based simulator across learning scenarios. In Agents and Data Mining Interaction, Editors: Cao L., Bazzan A., Symeonidis A., Gorodetsky V., Weiss, G., Yu P., LNCS 7103, Springer, 2012, pp. 86-97.
[26]R. Lungu, M. Lungu and C. Rotaru, Nonlinear adaptive system for the control of the helicopters pitch’s angle, Proceedings of the Romanian Academy, Series A: Mathematics, Physics, Technical Sciences, Information Science, vol.12, no.2, 2011, pp.133–142.
[27] M.I. Garcia-Planas, Sensitivity and stability of singular systems under proportional and derivative feedback, WSEAS Transactions on Mathematics, Vol.8, no.11, 2009,pp 635-644,.
[28]Q. G. Wang,Y. Zhang and M. S. Chiu, Decoupling internal Model Control for Multi-variable Systems with multiple time delays, Chemical Engineering, Vol.57, 2002, pp.115-124.
[29]Q. Xiong, W.J. Cai, Mao-Jun He, A practical loop pairing criterion for multivariable process, J. Process Control, Vol.15, 2005, pp.741-747.
[30]Q. G. Wang, C. C. Hang and B. Zou, A frequency response approach to autotuning of multivariable controllers, Chemical Engineering Research and Design, Vol,75, no.8, 1997, pp.797-806.

Table 1. Calculated results of a stable(Point Q_1) and an unstable limit-cycle(Point Q_3).

Point	$N_1(a_1)$	$N_2(a_2)$	ω	A_1	A_2	$\frac{\partial N_1(a_1)}{\partial A_1}$	$\frac{\partial N_2(a_2)}{\partial A_2}$	$\theta_2^{\{9\}}$	$\theta_2^{\{11\}}$	$M_{\theta 2}$
Q_1	0.3803	03803	0.7888	3.178	3.178	-0.107	-0.107	-70.87°	-70.87°	0.92
				1.054	1.054	+2.924*	+2.924*	-70.87°	-70.87°	0.92
Q_3	0.6366	0.2417	0.9595	1.420	1.019	0.000	+5.856*	-132.01	-132.28	0.66*
				1.420	5.168	0.000	-0.045	-131.98	-132.28	0.13*

Table 2. The gains k_m for just having a limit cycle.

Methods	Gain k_m
Proposed method	1.7915
Aizerman Conjecture	1.79
Hirsch plot	1.25
Mee plot	1.50
Digital Simulation	1.7885

Table 3. Calculated and Simulated Results for variable set of (k_1 , k_2).

Loop gains		**Calculated**			**Simulated**		
k_1	k_2	A_{1m}	A_{2m}	ω_c rad/s	A_{1s}	A_{2s}	ω_s rad/s
0.400	0.400	0.000	0.000	0.0000	0.000	0.000	0.000
0.597	0.597	1.470	1.359	0.7888	1.523	1.433	0.783
0.597	1.000	1.630	2.680	0.7888	1.800	2.808	0.803
1.000	0.597	2.803	1.581	0.7888	3.068	1.704	0.789
1.000	1.000	3.302	3.053	0.7888	3.309	3.032	0.790
1.000	5.000	3.374	15.674	0.7888	3.393	15.802	0.789
5.000	5.000	17.364	16.052	0.7888	17.578	15.952	0.787
1.000	10.000	3.376	31.371	0.7888	3.396	31.665	0.789
5.000	1.000	16.967	3.128	0.7888	17.205	3.070	0.789
10.000	1.000	33.957	3.130	0.7888	34.466	3.071	0.789

Table 4. Calculated and simulated results of Example 1 for $k_1 = k_2 = 1$.

	Osci. Freq(rad/s)		**Channel #1**	**Channel #2**	θ_2 **(deg)**	$M_{\theta 2}$
Calculation	0.4875	$N_{ic}(a_i)$	0.4541	0.2929	-53.3	0.95
		A_{ic}	1.0961	2.1390		
Simulation	0.4836	A_{is}	1.0607	2.2454	-54.4	----

Table 5. Calculated and simulated results of Example 1.

Loop gains		**Calculated**			**Simulated**		
k_1	k_2	A_{1m}	A_{2m}	ω_c rad/s	A_{1s}	A_{2s}	ω_s rad/s
0.4530	0.3700	----	----	----	0.4229	0.6101	0.4784
0.4541	0.3709	0.40000	0.6099	0.4875	0.4275	0.6175	0.4785
0.5000	0.5000	0.48994	1.0048	0.4875	0.5164	0.9880	0.4788
1.0000	1.0000	1.09609	2.1390	0.4875	1.0587	2.2447	0.4830
2.0000	2.0000	2.23103	4.3304	0.4875	2.1696	4.7227	0.4840
1.0000	10.000	1.09609	21.7318	0.4875	1.1075	24.5620	0.4839
10.000	1.0000	11.21309	2.1390	0.4875	10.5565	2.2443	0.4828
10.000	10.000	11.21309	21.7318	0.4875	11.0485	24.5620	0.4843

Table 6. Calculated and simulated results of Example 2.

Loop gains			**Calculated**				**Simulated**			
k_1	k_2	k_3	ω_c rad/s	A_{1C}	A_{2C}	A_{3C}	ω_s rad/s	A_{1S}	A_{2S}	A_{3S}
1.00	1.00	1.00	2.0606	2.552	2.552	2.552	2.145	2.832	2.832	2.832
1.00	1.00	2.00	2.0606	2.552	2.552	5.103	2.145	2.832	2.832	5.664
1.00	2.00	1.00	2.0606	2.552	5.110	2.552	2.145	2.832	5.664	2.832
0.50	0.50	0.50	2.0606	1.276	1.276	1.276	2.145	1.416	1.416	1.416
0.10	0.10	0.10	2.0606	0.2552	0.2552	0.2552	2.145	0.283	0.283	0.283
0.01	0.01	0.01	2.0606	0.02552	0.02552	0.02552	2.145	0.0283	0.0283	0.0283
0.10	1.00	5.00	2.0606	0.2552	2.552	12.758	2.145	0.283	2.832	14.160

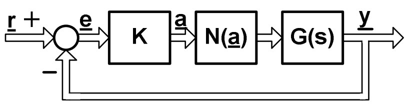

Fig.1. Nonlinear Multivariable Feedback Control System.

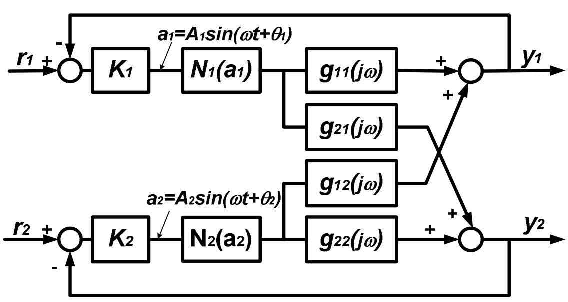

Fig.2. A 2x2 Nonlinear Multivariable Feedback Control System.

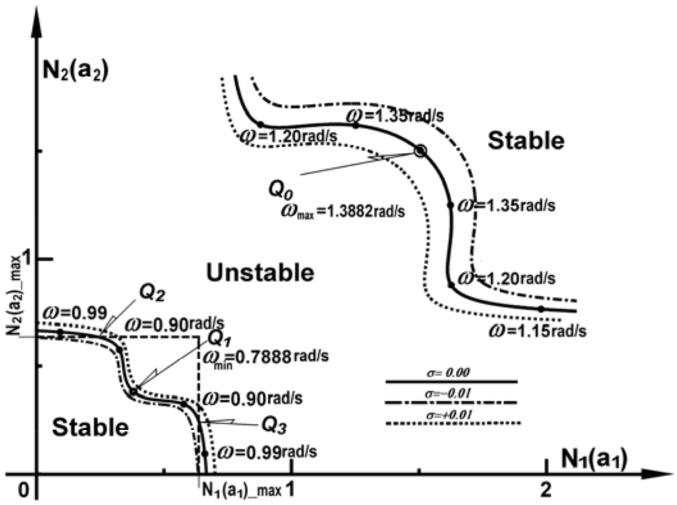

Fig.3. Root-Loci of limit cycles in the parameter plane.

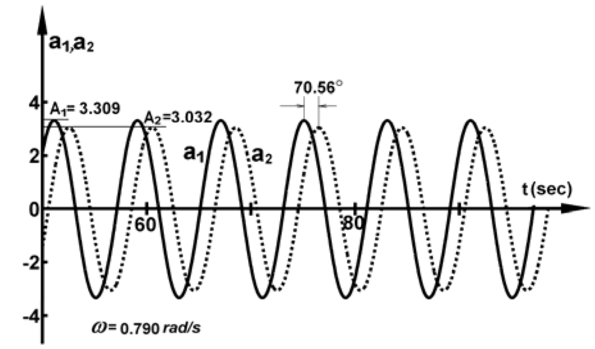

Fig.4. Time responses of the illustrating example.

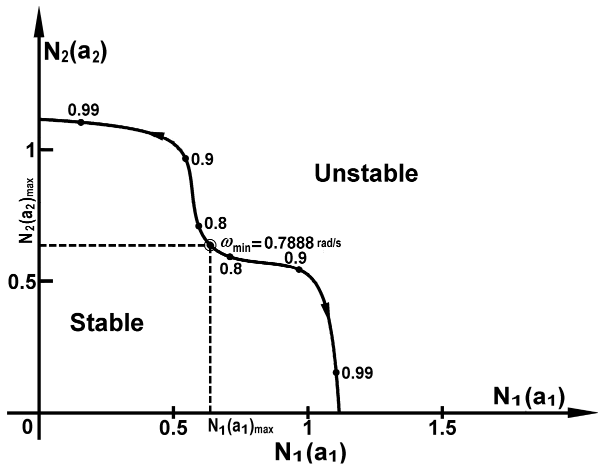

Fig.5. Root-locus analyses for k_m =1.7915.

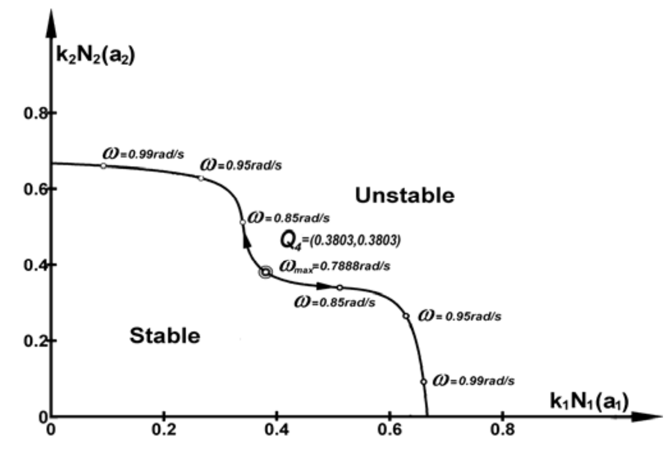

Fig.6. Root-Loci of limit cycles in the parameter plane.

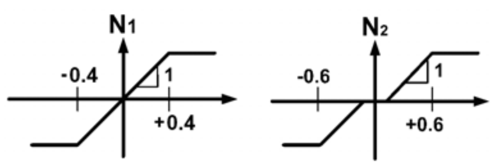

Fig.7. Nonlinearities of Example 1.

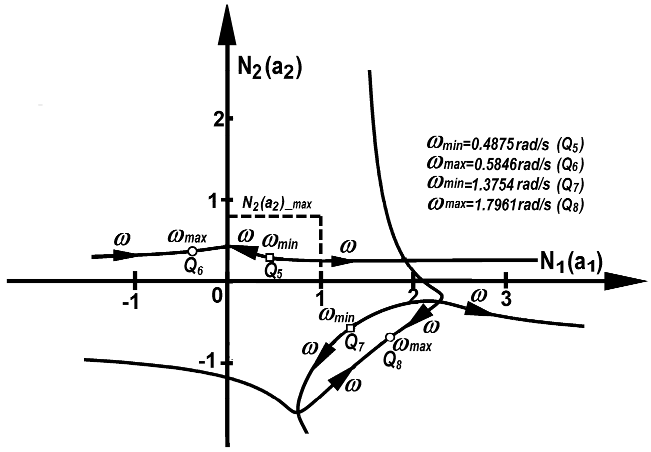

Fig.8. Root-loci Analyses of limit cycles of Example 1 for $k_1 = k_2 = 1$.

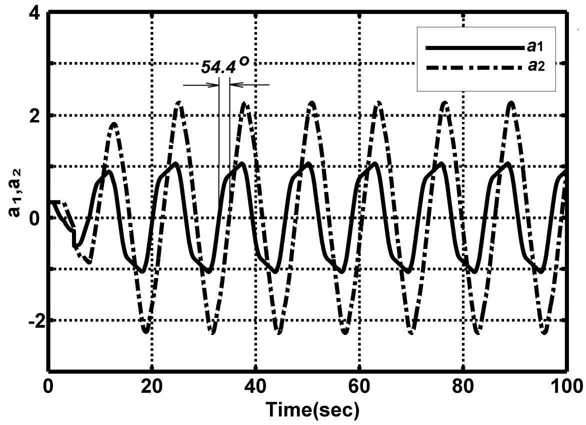

Fig.9. Time responses of Example 1 for $k_1 = k_2 = 1$.

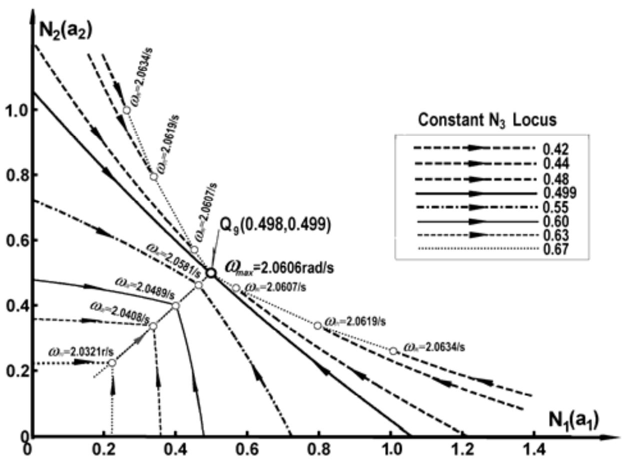

Fig.10. Root-loci analyses of limit cycles of Example 2 on $N_1(a_1)$ vs. $N_2(a_2)$ Plane for $N_3(a_3)$ varying and $k_i = 1$..

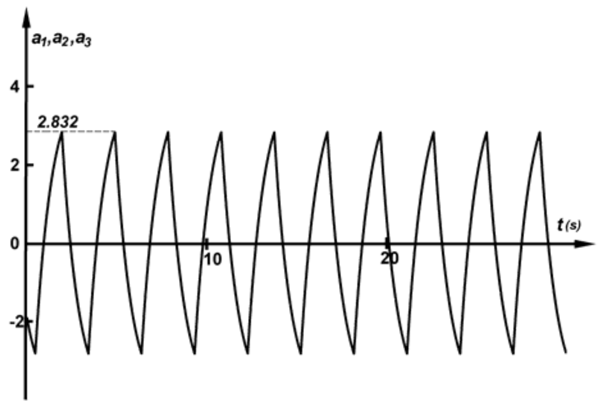

Fig.11. Time responses of Example 2 for $k_i = 1$.

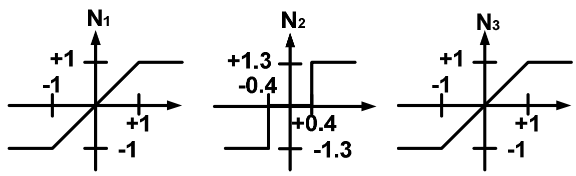

Fig.12. Nonlinearities of Example 3.

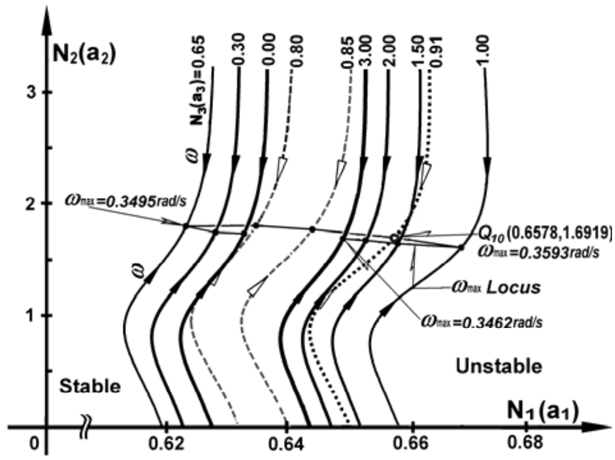

Fig.13(a). Root-loci analyses of limit cycles of Example 3 for $k_i = 1$.

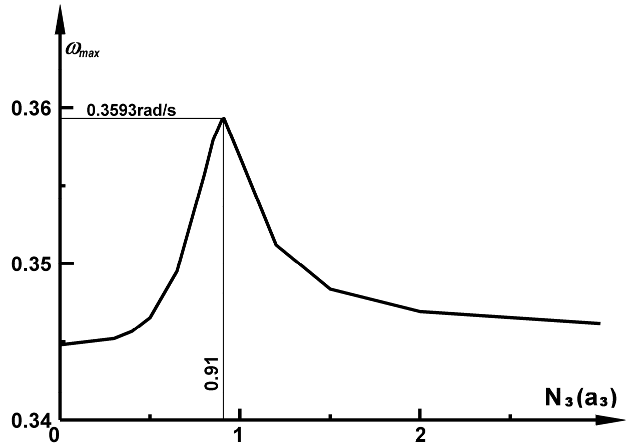

Fig.13(b). $\omega_{\max}$ -Locus of Example 3 for $k_i = 1$..

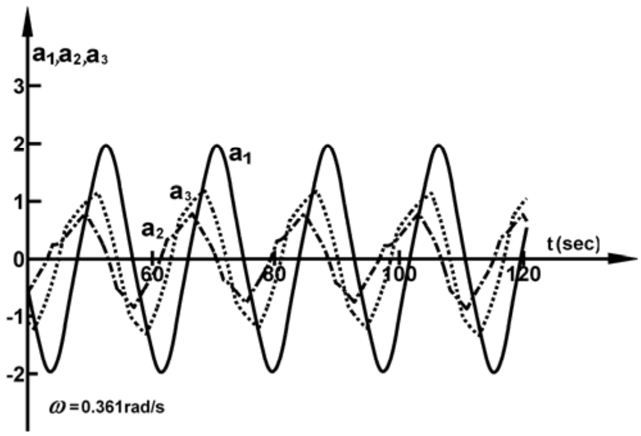

Fig.14. Time responses of Example 3 for $k_i = 1$..